
Decentralized Variational Bayesian Inference

Trevor Campbell
MIT
Cambridge, MA 02139
tdjc@mit.edu

Jonathan P. How
MIT
Cambridge, MA 02139
jhow@mit.edu

Abstract

This work presents a decentralized, approximate method for performing variational inference on a network of learning agents. The key difficulty with performing decentralized inference is that for most Bayesian models, the use of approximate inference algorithms is required, but such algorithms destroy symmetry and dependencies in the model that are crucial to properly combining the local models from each individual learning agent. This paper first investigates how approximate inference schemes break dependencies in Bayesian models. Using insights gained from that investigation, an optimization problem is proposed whose solution accounts for those broken dependencies when combining local posteriors. Experiments on synthetic and real data demonstrate that the decentralized method provides advantages in computational performance and predictive test likelihood over previous centralized and distributed methods.

1 INTRODUCTION

Recent trends in the growth of datasets, and the methods by which they are collected, have led to increasing interest in the parallelization of machine learning algorithms. Parallelization results in reductions in both the memory usage and computation time of learning, and allows data to be collected by a network of learning agents rather than by a single central agent. There are two major classes of parallelization algorithms: those that require a globally shared memory/computation unit (e.g., a central fusion processor that each learning agent is in communication with, or the main thread on a multi-threaded computer), and those that do not. While there is as of yet no consensus in the literature

on the terminology for these two types of parallelization, in this work we refer to these two classes, respectively, as *distributed* and *decentralized* learning.

Some recent approaches to distributed learning have involved using streaming variational approximations (Broderick et al., 2013), parallel stochastic gradient descent (Niu et al., 2011), the Map-Reduce framework (Dean and Ghemawat, 2004), database-inspired concurrency control (Pan et al., 2013), and message passing on graphical models (Gonzalez et al., 2009). When a reliable centralized learning agent with sufficient communication bandwidth is available, such distributed learning techniques are generally preferred to decentralized learning. This is a result of the consistent global model shared by all agents, with which they can make local updates without the concern of generating conflicts unbeknownst to each other.

Decentralized learning is a harder problem in general, due to asynchronous communication/computation, a lack of a globally shared state, and potential network and learning agent failure, all of which may lead to inconsistencies in the model possessed by each agent. Addressing these issues is particularly relevant to mobile sensor networks in which the network structure varies over time, agents drop out and are added dynamically, and no single agent has the computational or communication resources to act as a central hub during learning. Past approaches to decentralized learning typically involve each agent communicating frequently to form a consensus on the model over the network, and are often model-specific: particle filtering for state estimation (Rosencrantz et al., 2003) involves sending particle sets and informative measurements to peers; distributed EM (Wolfe et al., 2008) requires communication of model statistics to the network after each local iteration; distributed Gibbs sampling (Newman et al., 2007) involves model synchronization after each sampling step; robust distributed inference (Paskin and Guestrin, 2004) requires the formation of a spanning tree of nodes in the network and

message passing; asynchronous distributed learning of topic models (Asuncion et al., 2008) requires communication of model statistics to peers after each local sampling step; and hyperparameter consensus (Fraser et al., 2012) requires using linear network consensus on exponential family hyperparameters.

The method proposed in the present paper takes a different tack; each agent computes an approximate mean field variational posterior using only their local datasets, sends and receives statistics to and from other agents in the network asynchronously, and combines the posteriors locally on-demand. Building upon insights from previous work on distributed and decentralized inference (Broderick et al., 2013, Rosencrantz et al., 2003), a naïve version of this algorithm based on Bayes’ rule is presented. It is then shown that, due to the mean-field assumption of variational inference, this algorithm leads to poor decentralized posterior approximations for unsupervised models with inherent symmetry. Next, building on insights gained from the results of variational and Gibbs sampling inference on a synthetic example, an approximate posterior combination algorithm is presented that accounts for symmetry structure in models that the naïve algorithm is unable to capture. The proposed method is highly flexible, as it can be combined with past streaming variational approximations (Broderick et al., 2013, Lin, 2013), agents can share information with only subsets of the network, the network may be dynamic with unknown topology, and the failure of individual learning agents does not affect the operation of the rest of the network. Experiments on a mixture model, latent Dirichlet allocation (Blei et al., 2003), and latent feature assignment (Griffiths and Ghahramani, 2005) demonstrate that the decentralized method provides advantages in model performance and computational time over previous approaches.

2 APPROXIMATE DECENTRALIZED BAYESIAN INFERENCE

2.1 THE NAÏVE APPROACH

Suppose there is a set of learning agents i , $i = 1, \dots, N$, each with a distribution on a set of latent parameters θ_j , $j = 1, \dots, K$ (all parameters θ_j may generally be vectors). Suppose a mean field approximation with exponential family distributions has been used to approximate each agent’s posterior $q_i(\theta_1, \dots, \theta_K)$. Then the distribution possessed by each agent i is

$$q_i(\theta_1, \dots, \theta_K) = \prod_j q_{\lambda_{ij}}(\theta_j), \quad (1)$$

where λ_{ij} parameterizes agent i ’s distribution over θ_j . Given the prior

$$q_0(\theta_1, \dots, \theta_K) = \prod_j q_{\lambda_{0j}}(\theta_j), \quad (2)$$

is known by all agents, and the conditional independence of data given the model, the overall posterior distribution $q(\theta_1, \dots, \theta_K)$ may be approximated by using Bayes’ rule (Broderick et al., 2013) and summing over the λ_{ij} :

$$\begin{aligned} q(\cdot) &\propto q_0(\cdot)^{1-N} \prod_i q_i(\cdot) \\ &= \left(\prod_j q_{\lambda_{0j}}(\theta_j) \right)^{1-N} \prod_i \prod_j q_{\lambda_{ij}}(\theta_j) \\ \therefore q(\cdot) &= \prod_j q_{\lambda_j}(\theta_j) \end{aligned} \quad (3)$$

$$\text{where } \lambda_j = (1 - N)\lambda_{0j} + \sum_i \lambda_{ij}.$$

The last line follows from the use of exponential family distributions in the mean field approximation. This procedure is decentralized, as each agent can asynchronously compute its individual posterior approximation, broadcast it to the network, receive approximations from other agents, and combine them locally. Furthermore, this procedure can be made to handle streaming data by using a technique such as SDA-Bayes (Broderick et al., 2013) or sequential variational approximation (Lin, 2013) on each agent locally to generate the streaming local posteriors q_i .

As an example, this method is now applied to decentralized learning of a Gaussian model with unknown mean $\mu = 1.0$ and known variance $\sigma^2 = 1.0$. The prior on μ is Gaussian with mean $\mu_0 = 0.0$ and variance $\sigma_0^2 = 2.0$. There are 10 learning agents, each of whom receives 10 observations $y \sim \mathcal{N}(\mu, \sigma^2)$. Because the Gaussian distribution is in the exponential family, the mean field approximation is exact in this case. As shown in Figure 1, the decentralized posterior is the same as the centralized posterior. Note that if the mean field approximation is used on a more complicated distribution not in the exponential family, then the centralized estimate may in general differ from the decentralized estimate; however, they will both approximate the same true posterior distribution.

2.2 FAILURE OF THE NAÏVE APPROACH UNDER PARAMETER PERMUTATION SYMMETRY

As a second example, we apply decentralized inference to a Gaussian mixture model with three components having unknown means $\mu = (1.0, -1.0, 3.0)$ and

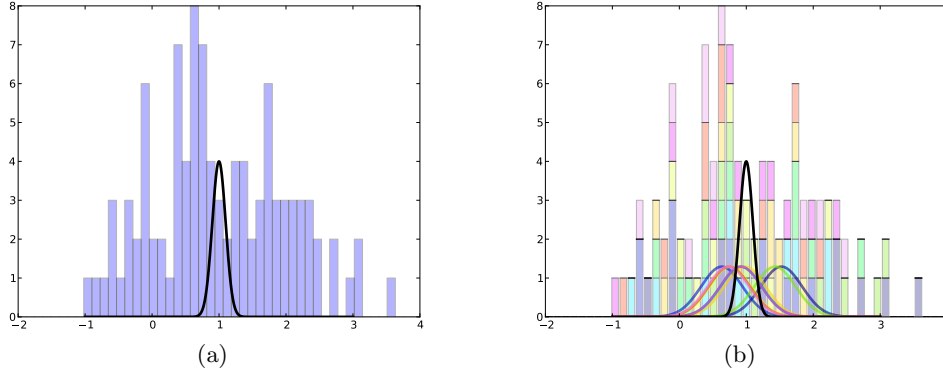


Figure 1: (1a): Centralized posterior of μ in black, with histogram of observed data. (1b): Decentralized posterior of μ in black, individual posteriors in color and correspondingly colored histogram of observed data.

cluster weights $\pi = (0.6, 0.3, 0.1)$ with known variance $\sigma^2 = 0.09$. The prior on each mean μ_i was Gaussian with mean $\mu_0 = 0.0$ and variance $\sigma_0^2 = 2.0$, while the prior on the weights π was Dirichlet with parameters $(1.0, 1.0, 1.0)$. First, the true posterior, shown in Figure 2a, was formed using 30 datapoints that were sampled from the generative model. Then, the decentralized variational inference procedure in (3) was run with 10 learning agents, each of whom received 3 of the datapoints, resulting in the approximate decentralized posterior in Figure 2b.

The decentralized posterior, in this case, is a very poor approximation of the true centralized posterior. The reason for this is straightforward: approximate inference algorithms, such as mean field variational inference, often do not capture *parameter permutation symmetry* in the posterior. Parameter permutation symmetry is a property of a Bayesian model in which permuting the values of some subset of the parameters does not change the posterior probability. For example, in the Gaussian mixture model, the true posterior over π, μ given data y is invariant to transformation by any permutation matrix P :

$$p(P\pi, P\mu|y) = p(\pi, \mu|y). \quad (4)$$

Indeed, examining the true posterior in Figure 2a, one can identify 6 differently colored regions; each of these regions corresponds to one of the possible $3! = 6$ permutation matrices P . In other words, the true posterior captures the invariance of the distribution to reordering of the parameters correctly.

To demonstrate that approximate inference algorithms typically do not capture parameter permutation symmetry in a model, consider the same mixture model, learned with 30 datapoints in a centralized manner using Gibbs sampling and variational Bayesian inference. Samples from 5 random restarts of each method are shown in Figure 3. Both algorithms fail to capture the permutation symmetry in the mixture model,

and converge to one of the 6 possible orderings of the parameters. This occurs in variational Bayesian inference and Gibbs sampling for different reasons: Gibbs sampling algorithms often get stuck in local posterior likelihood optima, while the mean field variational approximation explicitly breaks the dependence of the parameters on one another.

In a centralized setting, this does not pose a problem, because practitioners typically find the selection of a particular parameter ordering acceptable. However, in the decentralized setting, this causes problems when combining the posteriors of individual learning agents. If each agent effectively picks a parameter ordering at random when performing inference, combining the posteriors without considering those orderings can lead to disastrous results (such as that presented in Figure 2b).

2.3 MERGING POSTERiors WITH PARAMETER PERMUTATION SYMMETRY

This section presents a method for locally combining the individual posteriors of decentralized learning agents when the model contains parameter permutation symmetry. Formally, suppose that the true posterior probability of $\theta_1, \dots, \theta_K$ is invariant to permutations of the components of one or more θ_j . In general, there may be subsets of parameters which have coupled symmetry, in that the true posterior is only invariant if the components of all parameters in the subset are permuted in the same way (for example, the earlier Dirichlet mixture model had coupled permutation symmetry in μ and π). It is assumed that any such coupling in the model is known beforehand by all agents. Because the exponential family mean field variational approximation is completely decoupled, it is possible to treat each coupled permutation symmetry set of parameters in the model independently; therefore, we assume be-

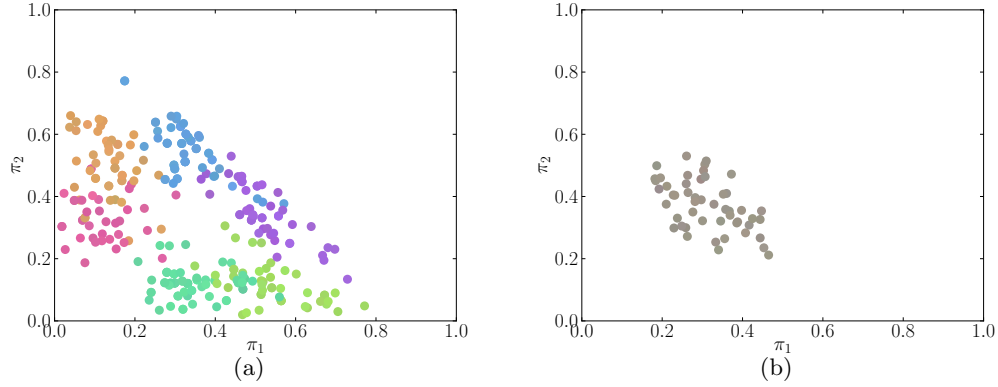


Figure 2: (2a): Samples from the true posterior over μ, π . Each particle’s position on the simplex (with $\pi_3 = 1 - \pi_1 - \pi_2$) represents the sampled weights, while RGB color coordinates of each particle represent the sampled position of the three means. (2b): Samples from the naively constructed decentralized approximate posterior, with the same coloring scheme. Note the disparity with Figure 2a.

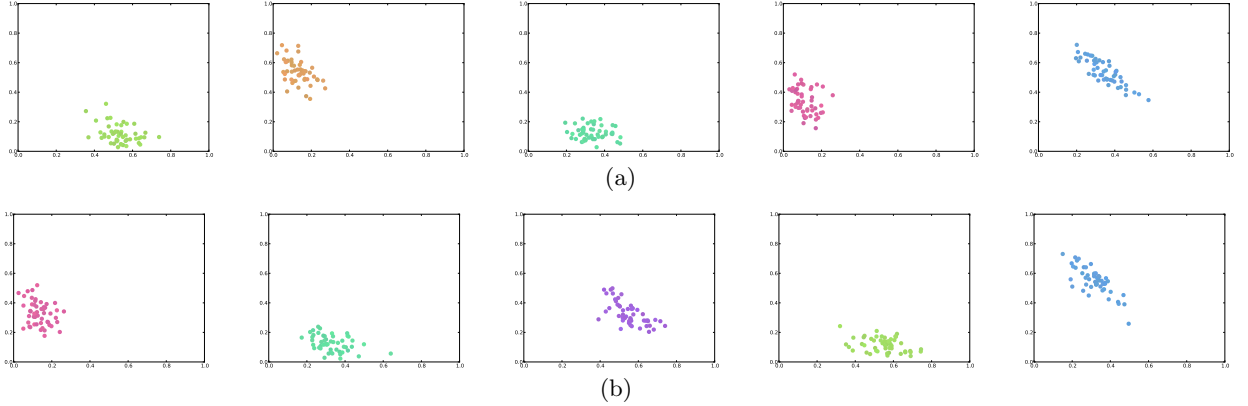


Figure 3: Centralized Gibbs sampling (3a) and variational Bayes (3b) approximate posterior samples from 5 random restarts. Comparison to Figure 2a shows that both approximate inference algorithms tend to converge to a random component of the permutation symmetry in the true posterior.

low that $\theta_1, \dots, \theta_K$ all have coupled permutation symmetry, for simplicity in the notation and exposition.

In order to properly combine the approximate posterior produced by each learning agent, first the individual posteriors are *symmetrized* (represented by a tilde) by summing over all possible permutations as follows:

$$\tilde{q}_i(\cdot) \propto \sum_{P_i} \prod_j q_{P_i \lambda_{ij}}(\theta_j), \quad (5)$$

where the sum over P_i is taken to be over all permutation operators on λ_{ij} . This process is referred to as symmetrization because \tilde{q}_i has the same parameter permutation symmetry as the true posterior, i.e. for all permutation matrices P ,

$$\tilde{q}_i(P\theta_1, \dots, P\theta_K) = \tilde{q}_i(\dots). \quad (6)$$

To demonstrate the effect of this procedure, the mixture model example was rerun with centralized variational Bayesian inference (i.e. all 30 datapoints were given to a single learner) followed by symmetrization. Samples generated from these new symmetrized pos-

terior distributions over 5 random restarts of the inference procedure are shown in Figure 4. This result demonstrates that the symmetrized distributions are invariant to the random permutation to which the original approximate posterior converged.

It is now possible to combine the individual (symmetrized) posteriors via the procedure outlined in (3):

$$\begin{aligned} q(\cdot) &\propto q_0(\cdot)^{1-N} \prod_i \tilde{q}_i(\cdot) \\ &= \left(\prod_j q_{\lambda_{0j}}(\theta_j) \right)^{1-N} \prod_i \sum_{P_i} \prod_j q_{P_i \lambda_{ij}}(\theta_j) \quad (7) \\ &= \sum_{\{P_i\}_i} \prod_j \left[q_{\lambda_{0j}}(\theta_j)^{1-N} \prod_i q_{P_i \lambda_{ij}}(\theta_j) \right], \end{aligned}$$

where the outer sum is now over unique combinations of the set of permutation operators $\{P_i\}_i$ used by the learning agents.

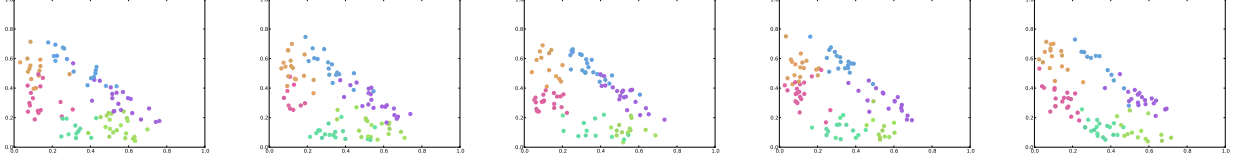


Figure 4: Samples from the symmetrized centralized variational Bayes approximate posterior from 5 random restarts. Comparison to Figure 2a shows that symmetrization reintroduces the structure of the true posterior to the approximate posteriors.

2.4 AMPS - APPROXIMATE MERGING OF POSTERIOR WITH SYMMETRY

The posterior distribution in (7) is unfortunately intractable to use for most purposes, as it contains a number of terms that is factorial in the dimensions of the parameters, and exponential in the number of learning agents. Therefore, we approximate this distribution by finding the component with the highest weight – the intuitive reasoning for this is that the component with the highest weight is the one for which the individual posteriors have correctly aligned permutations, thus contributing to each other the most and representing the overall posterior the best. While the resulting distribution will not be symmetric, it will appear as though it were generated from variational Bayesian inference; this, as mentioned before, is most often fine in practice.

In order to compute the weight of each component, we need to compute its integral over the parameter space. Suppose that each mean field component $q_{\lambda_{ij}}(\theta_j)$ has the following form:

$$q_{\lambda_{ij}}(\theta_j) = h_j(\theta_j) e^{\text{tr}[\lambda_{ij}^T T(\theta_j)] - A_j(\lambda_{ij})} \quad (8)$$

where h_j and A_j are the base measure and log-partition functions for parameter j , respectively. The trace is used in the exponent in case λ_{ij} is specified as a matrix rather than as a single column vector (such as in the example presented in Section 3.1). Thus, given a set of permutation operators $\{P_i\}_i$, the factor of the weight for the component due to parameter j is

$$W_j(\{P_i\}_i) = \int_{\theta_j} q_{\lambda_{0j}}(\theta_j)^{1-N} \prod_i q_{P_i \lambda_{ij}}(\theta_j). \quad (9)$$

The overall weight of the component is the product over the parameters, so finding the maximum weight component of (7) is equivalent to finding the set of permutation operators P_i^* that maximizes the product of the W_j ,

$$\{P_i^*\}_i \leftarrow \arg \max_{\{P_i\}_i} \prod_j W_j(\{P_i\}_i). \quad (10)$$

Due to the use of exponential family distributions in the mean field approximation, the optimization (10)

can be posed as a combinatorial optimization over permutation matrices with a closed-form objective:

$$\begin{aligned} \max_{P_i} \sum_j A_j \left((1-N)\lambda_{0j} + \sum_i P_i \lambda_{ij} \right) \\ \text{s.t. } P_i \in S \quad \forall i \end{aligned} \quad (11)$$

where S is the symmetric group of order equal to the row dimension of the matrices λ_{ij} . Alternatively, if it is more convenient for the particular form of A_j , one can reformulate (10) as a convex maximization over a polytope,

$$\begin{aligned} \max_{z_{ik}} \sum_j A_j \left((1-N)\lambda_{0j} + \sum_{i,k} z_{ik} \lambda_{ij}^{(k)} \right) \\ \text{s.t. } \sum_k z_{ik} = 1 \quad \forall i \\ z_{ik} \geq 0 \quad \forall i, k \end{aligned} \quad (12)$$

using the convexity of the objective, the fact that the objective is affine in its arguments, and the total unimodularity of the constraint polytope, where $\lambda_{ij}^{(k)}$ is one of the possible permutations of the rows of λ_{ij} . Global optimization routines for this problem are intractable for the problem sizes presented by typical Bayesian models (Benson, 1985, Falk and Hoffman, 1986). Thus, the optimization must be solved approximately, where the choice of the approximate method is dependent on the particular form of A_j .

As mentioned earlier, this optimization was formulated assuming that all the θ_j were part of a single coupled permutation symmetry set. However, if there are multiple subsets of the parameters $\theta_1, \dots, \theta_K$ that have coupled permutation symmetry, an optimization of the form (12) can be solved for each subset independently. In addition, for any parameter that does not exhibit permutation symmetry, the original naïve posterior merging procedure in (3) may be used. These two statements follow from the exponential family mean field assumption used to construct the individual approximate posteriors q_i .

3 EXPERIMENTS

All experiments were performed on a computer with an Intel Core i7 processor and 12GB of memory.

3.1 DECENTRALIZED MIXTURE MODEL EXAMPLE REVISITED

The AMPS decentralized inference scheme was applied to the Gaussian mixture model example from earlier, with three components having unknown means $\mu = (1.0, -1.0, 3.0)$ and cluster weights $\pi = (0.6, 0.3, 0.1)$, and known variance $\sigma^2 = 0.09$. The prior on each mean μ_i was Gaussian, with mean $\mu_0 = 0.0$ and variance $\sigma_0^2 = 2.0$, while the prior on the weights π was Dirichlet, with parameters $(1.0, 1.0, 1.0)$. The dataset consisting of the same 30 datapoints from the earlier trial was used, where each of 10 learning agents received 3 of the datapoints. Each learning agent used variational Bayesian inference to find their individual posteriors $q_i(\mu, \pi)$, and then used AMPS to merge them. The only communication required between the agents was a single broadcast of each agent's individual posterior parameters.

In this example, the AMPS objective¹ was as follows:

$$J_{\text{AMPS}} = -\log \Gamma \left(\sum_{j=1}^3 (\beta_j + 1) \right) + \sum_{j=1}^3 -\frac{\eta_j^2}{4\nu_j} - \frac{1}{2} \log(-2\nu_j) + \log \Gamma(\beta_j + 1) \quad (13)$$

with

$$\begin{aligned} \lambda_{i\mu} &= \begin{bmatrix} \eta_{i1} & \eta_{i2} & \eta_{i3} \\ \nu_{i1} & \nu_{i2} & \nu_{i3} \end{bmatrix}^T, \quad i = 1, \dots, 10 \\ \lambda_{i\pi} &= \begin{bmatrix} \beta_{i1} & \beta_{i2} & \beta_{i3} \end{bmatrix}^T, \quad i = 1, \dots, 10 \\ \lambda_{\mu} &= -9\lambda_{0\mu} + \sum_i P_i \lambda_{i\mu} \equiv \begin{bmatrix} \eta_1 & \eta_2 & \eta_3 \\ \nu_1 & \nu_2 & \nu_3 \end{bmatrix}^T \\ \lambda_{\pi} &= -9\lambda_{0\pi} + \sum_i P_i \lambda_{i\pi} \equiv \begin{bmatrix} \beta_1 & \beta_2 & \beta_3 \end{bmatrix}^T \quad (14) \\ \lambda_{0\mu} &= \begin{bmatrix} 0 & 0 & 0 \\ -0.25 & -0.25 & -0.25 \end{bmatrix}^T \\ \lambda_{0\pi} &= \begin{bmatrix} 0 & 0 & 0 \end{bmatrix}^T \\ \beta_{ij} &= \alpha_{ij} - 1, \quad \eta_{ij} = \frac{\mu_{ij}}{\sigma_{ij}^2}, \quad \nu_{ij} = -\frac{1}{2\sigma_{ij}^2} \end{aligned}$$

where α_{ij} was agent i 's posterior Dirichlet variational parameter for cluster j , and μ_{ij}/σ_{ij}^2 were agent i 's pos-

terior normal variational parameter for cluster j . The objective was optimized approximately over the 3×3 permutation matrices P_i by proposing swaps of two rows in P_i , accepting swaps that increased J_{AMPS} , and terminating when no possible swaps increased J_{AMPS} .

The individual posteriors for 3 of the learning agents are shown in Figure 5, while the decentralized posterior over all the agents is shown in Figure 6 alongside its symmetrization (for comparison to the true posterior – this final symmetrization is not required in practice). The AMPS posterior is a much better approximation than the naïve decentralized posterior shown in Figure 2b; this is because the AMPS posterior accounts for parameter permutation symmetry in the model prior to combining the individual posteriors. It may be noted that the decentralized posterior has slightly more uncertainty in it than the centralized posterior, but this is to be expected when each learning agent individually receives little information (as demonstrated by the uncertainty in the individual posteriors shown in Figure 5).

3.2 DECENTRALIZED LATENT DIRICHLET ALLOCATION

The next experiment involved running decentralized variational inference with AMPS on the LDA document clustering model (Blei et al., 2003). The dataset in consideration was the 20 newsgroups dataset, consisting of 18,689 documents with 1,000 held out for testing, and a vocabulary of 11,175 words after removing stop words and stemming the remaining words. Algorithms were evaluated based on their approximate predictive likelihood of 10% of the words in each test document given the remaining 90%, as described in earlier literature (Wang et al., 2011). The variational inference algorithms in this experiment were initialized using smoothed statistics from randomly selected documents.

In LDA, the parameter permutation symmetry lies in the arbitrary ordering of the global word distributions for each topic. In particular, for the 20 newsgroups dataset, decentralized learning agents may learn the 20 Dirichlet distributions with a different ordering; therefore, in order to combine the local posteriors, we use AMPS with the following objective to reorder each agent's global topics:

$$J_{\text{AMPS}} = \sum_{k=1}^K J_{\text{AMPS},k} = \sum_{k=1}^K \sum_{w=1}^W \log \Gamma(\alpha_{kw}) - \log \Gamma \left(\sum_{w=1}^W \alpha_{kw} \right) \quad (15)$$

¹The AMPS objective for each experiment was constructed using the log-partition function $A_j(\cdot)$ of the relevant exponential family models, which may be found in (Nielsen and Garcia, 2011).

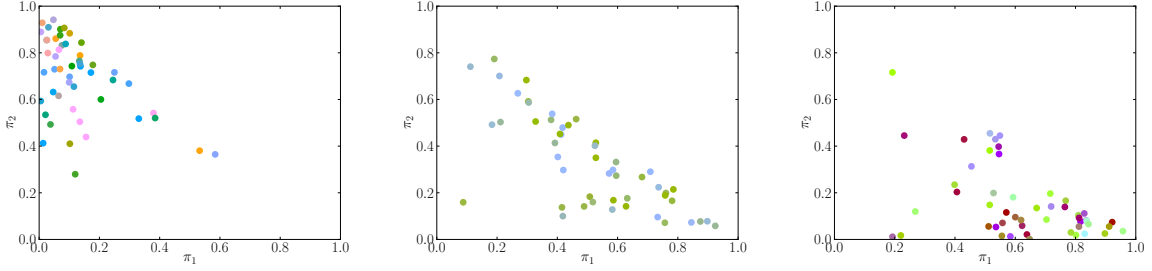


Figure 5: Samples from the individual posterior distributions from variational Bayesian inference for 3 of the learning agents. Note the high level of uncertainty in both the weights (position) and cluster locations (colour) in each posterior.

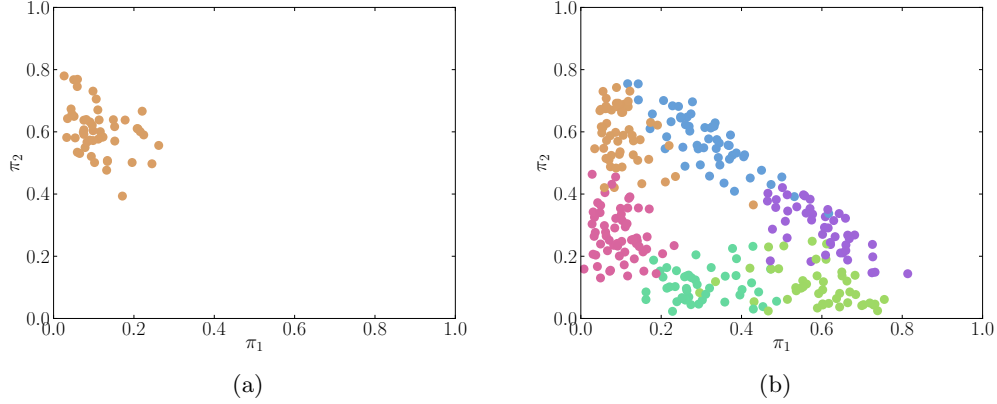


Figure 6: (6a): Samples from the decentralized posterior output by AMPS. Comparison to Figure 5 shows that the AMPS posterior merging procedure improves the posterior possessed by each agent significantly. (6b): Samples from the symmetrized decentralized posterior. This final symmetrization step is not performed in practice; it is simply done here for comparison with Figure 2a.

$$\alpha = (1 - N)\alpha_0 + \sum_{i=1}^N P_i \alpha_i, \quad \alpha, \alpha_i \in \mathbb{R}^{K \times W}$$

$$\alpha_{0kw} = \frac{10}{W} \quad K = 20, \quad W = 11, 175$$

where α_{ikw} is agent i 's posterior Dirichlet variational parameter for topic k and word w , and the optimization is over $K \times K$ permutation matrices $P_i, i = 1, \dots, N$. For the LDA model, the AMPS objective J_{AMPS} is additive over the topics k ; therefore, J_{AMPS} can be optimized approximately by iteratively solving maximum-weight bipartite matching problems as follows:

1. Initialize the decentralized posterior parameter $\alpha \leftarrow (1 - N)\alpha_0 + \sum_{i=1}^N P_i \alpha_i$ with a set of P_i matrices
2. For each agent i until J_{AMPS} stops increasing:
 - (a) Deassign agent i 's posterior: $\alpha \leftarrow \alpha - P_i \alpha_i$
 - (b) Form a bipartite graph with decentralized topics k on one side, agent i 's topics k' on the other, and edge weights $w_{kk'}$ equal to $J_{\text{AMPS},k}$ if agent i 's topic k' is assigned to the decentralized topic k

- (c) $P_i \leftarrow$ Maximum weight assignment of agent i 's topics
- (d) Reassign agent i 's posterior: $\alpha \leftarrow \alpha + P_i \alpha_i$

First, the performance of decentralized LDA with AMPS was compared to the centralized approximate LDA posterior with a varying number of learning agents. Figure 7 shows the test data log likelihood and computation time over 20 trials for the centralized posterior, the AMPS decentralized posterior, and each individual agent's posterior for 5, 10, and 50 learning agents. The results mimic those of the synthetic experiment – the posterior output by AMPS significantly outperforms each individual agent's posterior, and the effect is magnified as the number of agents increases. Further, there is a much lower variance in the AMPS posterior test log likelihood than for each individual agent. The centralized method tends to get stuck in poor local optima in the variational objective, leading to relatively poor performance, while the decentralized method avoids these pitfalls by solving a number of smaller optimizations and combining the results afterwards with AMPS. Finally, as the number of agents increases, the amount of time required to solve the AMPS optimization increases; reducing this computa-

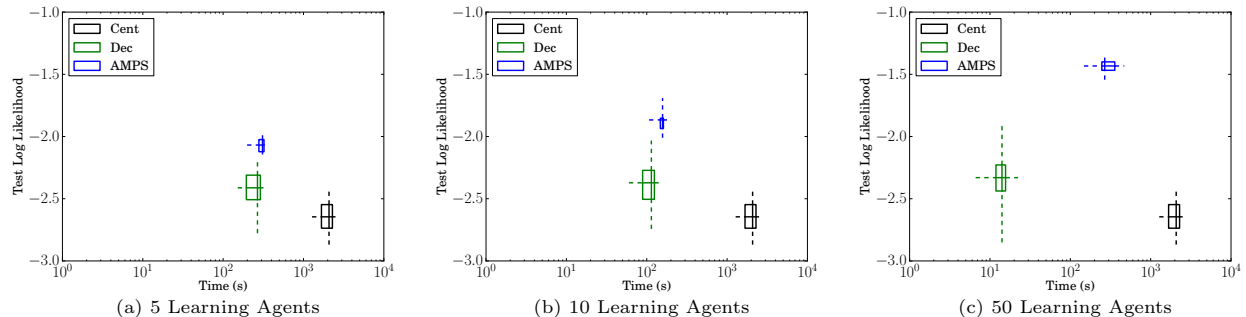


Figure 7: Plots of log likelihood on the test data for 5 (7a), 10 (7b), and 50 (7c) learning agents. The boxes bound the 25th and 75th percentiles of the data with medians shown in the interior, and whiskers show the maximum and minimum values.

tion time is a potential future goal for research on this inference scheme.

The next test compared the performance of AMPS to SDA-Bayes (Broderick et al., 2013), a recent streaming, distributed variational inference algorithm. The algorithms were tested on 20 trials of each of three settings: one with 1 agent and 10 subbatches of data per agent; one with 10 agents and 1 subbatch of data per agent; and finally, one with 10 agents and 10 subbatches of data per agent. Each agent processed its subbatches in serial. For SDA-Bayes, each agent updated a single distributed posterior after each subbatch. For the decentralized method, each agent used AMPS to combine the posteriors from its own subbatches, and then used AMPS again to combine each agent’s resulting posterior.

Figure 8 shows the results from this procedure. AMPS outperforms SDA-Bayes in terms of test log likelihood, and is competitive in terms of the amount of time it takes to perform inference and then optimize the AMPS objective. This occurs because AMPS takes into account the arbitrary ordering of the topics, while SDA-Bayes ignores this when combining posteriors. An interesting note is that the AMPS10x10 result took less time to compute than the time for 50 agents in Figure 7c, despite the fact that it effectively merged 100 posterior distributions; this hints that developing a hierarchical optimization scheme for AMPS is a good avenue for further exploration. A final note is that using AMPS as described above is not truly a streaming procedure; however, one can rectify this by periodically merging posteriors using AMPS to form the prior for inference on subsequent batches.

3.3 DECENTRALIZED LATENT FEATURE ASSIGNMENT

The last experiment involved running decentralized variational inference with AMPS on a finite latent feature assignment model (Griffiths and Ghahramani, 2005). In this model, a set of K feature vectors $\mu_k \in$

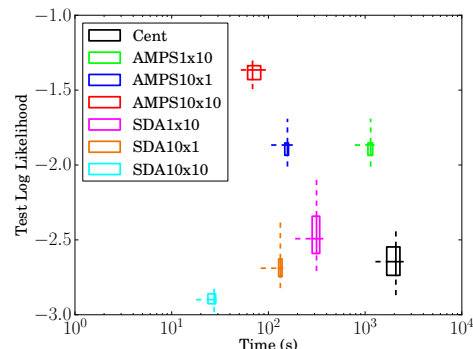


Figure 8: Comparison with SDA-Bayes. The $A \times B$ in the legend names refer to using A learning agents, where each splits their individual batches of data into B subbatches.

\mathbb{R}^D are sampled from a Gaussian prior $\mu_k \sim \mathcal{N}(0, \sigma_0^2 I)$, and a set of feature inclusion probabilities are sampled from a beta prior $\pi_k \sim \text{Beta}(\alpha_k, \beta_k)$. Finally, for each image i , a set of features z_i are sampled independently from the weights $z_{ik} \sim \text{Be}(\pi_k)$, and the image $y_i \in \mathbb{R}^D$ is sampled from a Gaussian likelihood $y_i \sim \mathcal{N}(\sum_k \mu_k z_{ik}, \sigma^2 I)$.

Two datasets were used in this experiment. The first was a synthetic dataset with $K = 5$ randomly generated $D = 10$ -dimensional binary feature vectors, feature weights sampled uniformly, and 1300 observations sampled with variance $\sigma^2 = 0.04$, with 300 held out for testing. For this dataset, algorithms were evaluated based on the error between the means of the feature posteriors and the true set of latent features, and based on their approximate predictive likelihoods of a random component in each test observation vector given the other 9 components. The second dataset was a combination of the Yale (Belhumeur et al., 1997) and Caltech² faces datasets, with 581 32×32 frontal images of faces, where 50 were held out for testing. The number of latent features was set to $K = 10$. For this dataset, algorithms were evaluated based on their approximate predictive likelihood of 10% of the pixels

²Available online: <http://www.vision.caltech.edu/html-files/archive.html>

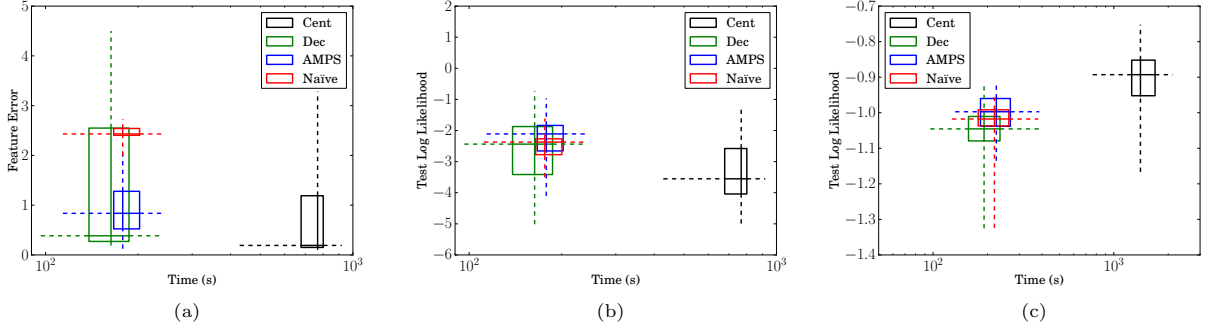


Figure 9: (9a): 2-norm error between the discovered features and the true set for the synthetic dataset. (9b): Test log likelihood for the synthetic dataset. (9c): Test log likelihood on the faces dataset. All distributed/decentralized results were generated using 5 learning agents.

in each test image given the remaining 90%, and the inference algorithms were initialized using smoothed statistics from randomly selected images.

The parameter permutation symmetry in the posterior of the latent feature model lies in the ordering of the features μ_k and weights π_k . Therefore, to combine the local posteriors, we use AMPS with the following objective to reorder each agent’s set of features and weights:

$$J_{\text{AMPS}} = \sum_{k=1}^K J_{\text{AMPS},k} = \sum_{k=1}^K \log \Gamma(\alpha_k) + \log \Gamma(\beta_k) - \log \Gamma(\alpha_k + \beta_k) - \frac{\eta_k^T \eta_k}{4\nu_k} - \frac{D}{2} \log(-2\nu_k) \quad (16)$$

where $\alpha, \beta \in \mathbb{R}^K$ are the combined posterior beta natural parameters, and $\eta \in \mathbb{R}^{D \times K}, \nu \in \mathbb{R}^K$ are the combined posterior normal natural parameters (combined using the $(1-N) *_0 + \sum_i P_i *_i$ rule as described in the foregoing). The priors were $\alpha_{k0} = \beta_{k0} = 1$, $\eta_{k0} = 0 \in \mathbb{R}^D$, and ν_{k0} was estimated from the data. As in the LDA model, the AMPS objective for the latent feature model is additive over the features k ; therefore the optimization was performed using iterative maximum-weight bipartite matchings as described in Section 3.2.

Figure 9 shows the results from the two datasets using centralized learning and decentralized learning. For the decentralized results, the posteriors of 5 learning agents were combined using AMPS or the naïve approach (equivalent to SDA5×1 in the notation of Figure 8). Figure 9a shows that AMPS discovers the true set of latent features with a lower 2-norm error than both the naïve posterior combination and the individual learning agents, with a comparable error to the centralized learning case. However, as shown in Fig-

ures 9b (synthetic) and 9c (faces), AMPS only outperforms the naïve approach in terms of predictive log likelihoods on the held-out test set by a small margin. This is due to the flexibility of the latent feature assignment model, in that there are many sets of latent features that explain the observations well.

4 DISCUSSION

This work introduced the Approximate Merging of Posteriors with Symmetry (AMPS) algorithm for approximate decentralized variational inference. AMPS may be used in ad-hoc, asynchronous, and dynamic networks. Experiments demonstrated the modelling and computational advantages of AMPS with respect to centralized and distributed learning. Motivated by the examples in Section 3, there is certainly room for improvement of the AMPS algorithm. For example, it may be possible to reduce the computational cost of AMPS by using a hierarchical optimization scheme rather than the monolithic approach used in most of the examples presented in the foregoing. Further, extending AMPS for use with Bayesian nonparametric models is of interest for cases when the number of latent parameters is unknown a priori, or when there is the possibility that agents learn disparate sets of latent parameters that are not well-combined by optimizing over permutations. Finally, while the approximate optimization algorithms presented herein work well in practice, it would be of interest to find bounds on the performance of such algorithms with respect to the true AMPS optimal solution.

References

- A. Asuncion, P. Smyth, and M. Welling. Asynchronous distributed learning of topic models. In *Advances in Neural Information Processing Systems 21*, 2008.
- P. Belhumeur, J. Hespanha, and D. Kriegman. Eigenfaces vs. fisherfaces: Recognition using class specific linear projection. *IEEE Trans. on Pattern Analysis in Machine Intelligence*, 19:711–720, 1997.

- H. P. Benson. A finite algorithm for concave minimization over a polyhedron. *Naval Research Logistics Quarterly*, 32(1):165–177, 1985.
- D. M. Blei, A. Y. Ng, and M. I. Jordan. Latent dirichlet allocation. *Journal of Machine Learning Research*, 3: 993–1022, 2003.
- T. Broderick, N. Boyd, A. Wibisono, A. C. Wilson, and M. I. Jordan. Streaming variational bayes. In *Advances in Neural Information Processing Systems 26*, 2013.
- J. Dean and S. Ghemawat. Mapreduce: Simplified data processing on large clusters. In *6th Symposium on Operating Systems Design and Implementation*, 2004.
- J. E. Falk and K. L. Hoffman. Concave minimization via collapsing polytopes. *Operations Research*, 34(6):919–929, 1986.
- C. S. Fraser, L. F. Bertuccelli, H.-L. Choi, and J. P. How. A hyperparameter consensus method for agreement under uncertainty. *Automatica*, 48:374–380, 2012.
- J. E. Gonzalez, Y. Low, and C. Guestrin. Residual splash for optimally parallelizing belief propagation. In *Proceedings of the 12th International Conference on Artificial Intelligence and Statistics*, 2009.
- T. L. Griffiths and Z. Ghahramani. Infinite latent feature models and the indian buffet process. In *Advances in Neural Information Processing Systems 22*, 2005.
- D. Lin. Online learning of nonparametric mixture models via sequential variational approximation. In *Advances in Neural Information Processing Systems 26*, 2013.
- D. Newman, A. Asuncion, P. Smyth, and M. Welling. Distributed inference for latent dirichlet allocation. In *Advances in Neural Information Processing Systems 20*, 2007.
- F. Nielsen and V. Garcia. Statistical exponential families: A digest with flash cards. *arXiv:0911.4853v2*, 2011.
- F. Niu, B. Recht, C. Ré, and S. J. Wright. Hogwild!: A lock-free approach to parallelizing stochastic gradient descent. In *Advances in Neural Information Processing Systems 24*, 2011.
- X. Pan, J. Gonzalez, S. Jegelka, T. Broderick, and M. I. Jordan. Optimistic concurrency control for distributed unsupervised learning. In *Advances in Neural Information Processing Systems 26*, 2013.
- M. A. Paskin and C. E. Guestrin. Robust probabilistic inference in distributed systems. In *Proceedings of the 20th Conference on Uncertainty in Artificial Intelligence*, 2004.
- M. Rosencrantz, G. Gordon, and S. Thrun. Decentralized sensor fusion with distributed particle filters. In *Proceedings of the 19th Conference on Uncertainty in Artificial Intelligence*, 2003.
- C. Wang, J. Paisley, and D. M. Blei. Online variational inference for the hierarchical dirichlet process. In *Proceedings of the 11th International Conference on Artificial Intelligence and Statistics*, 2011.
- J. Wolfe, A. Haghighi, and D. Klein. Fully distributed EM for very large datasets. In *Proceedings of the 25th International Conference on Machine Learning*, 2008.